J. Phys.: Condens. Matter 6 (1994) 5647–5656. Printed in the UK

Stability of a self-trapping hole in α-quartz

X Zhang†, C K Ong† and A M Stoneham‡

† Department of Physics, National University of Singapore, Singapore 0511

‡ AEA Industrial Technology, Harwell Laboratory, Didcot, Oxford OX11 0RA, UK

Received 29 March 1994

Abstract. Previous calculations of self-trapping in quartz adopt quantum chemical methods. However, for certain purposes, for example, when more than a few atoms are involved in a defect process, it would be helpful to use instead the shell model methods which work well for halides. We present the first calculation of the self-trapped hole (STH) in α-quartz and other forms of silicon dioxide using the classic defect simulation technique. The calculation suggests that the hole can be self-trapped on oxygen atom with a binding energy of 0.41 eV. The self-trapping is accompanied by a large network distortion, in which the O^- ion on which the hole is self-trapped shifts 0.14 Å and the nearest-neighbour silicon atoms move 0.4–0.6 Å away from the O^- ion. These results are similar to those obtained from the *ab initio* HF calculation of STH in amorphous SiO_2. We have also estimated the effective activation energy of a STH to be 0.12 eV at 180 K though there will also be a significant component of conduction from excitation of the small polaron to the delocalized large-polaron state.

1. Introduction

Self-trapping is a widespread phenomenon in insulators [1, 2]. As Landau first recognized [3], when there is strong electron–phonon coupling, the state of lowest energy for a carrier can be localized; in essence, the energy gain from deforming the host solid is greater than the energy cost of confining the carrier to a small volume. In a number of systems, the balance between the major energies is delicate. One such is silicon dioxide, whether quartz or some other structure. The exciton certainly self-traps, and this is the basis of the characteristic blue luminescence, with its very large Stokes shift from the ultraviolet band edge absorption. The rather small perturbations of Ge substituting for Si cause both electrons and holes to localize [4]. In the amorphous silicas, self-trapped holes have been identified, and the structural variations will be a contributing factor. Near to the interface of thermal oxide with the silicon substrate, the image interaction will favour localization because of the larger polarizability of Si. This case is of broader interest because the hopping of carriers between the Si and insulating oxide is one of the sources of electrical noise, and it is an open question as to whether the transfer is to a well-defined defect in the oxide or simply to a self-trapped state [5].

The theory of self-trapping in silicon dioxide has concentrated on quantum chemical methods at several levels of sophistication. These have clarified many issues and provide a firm basis for much of the experimental data. However, the computer needs for quantum chemistry are substantial, and these calculations have used relatively small clusters of atoms. What we attempt in this paper is a study by the simpler methods, based on the shell model and interatomic potentials. What we find are predictions in acceptable accord with both quantum chemistry and with experiment. This, in turn, means that we may sensibly apply

0953-8984/94/295647+10$19.50

these Mott–Littleton techniques to a variety of important problems in which the oxide is on a silicon substrate. For example, the methods could be used to study certain of the defect reactions involving the P_b centres [6, 7], the characteristic silicon dangling bond defects at silicon/thermal oxide interfaces.

Our present work concentrates on two fundamental questions that have yet to be satisfactorily answered. First, what is the type of trapped charge, i.e. does a trapped charge exist as a self-trapped hole (STH) or as a self-trapped electron (STE)? Secondly, how do these free carriers (not associated with impurities or structural defects) migrate in quartz? We shall concentrate on the problems of the STH since the study of STE involves the conduction band of the SiO_2 and reliable results are not available with the current methods.

Experimental evidence for the STH in SiO_2 comes mainly from ESR experiments; data for the STE come from optical and associated methods. Hayes and Jenkin [8] identified a STH in germanium-doped α-quartz, but were unable to find a STH in undoped α-quartz. Griscom [9] observed two ESR spectra (STH_1 and STH_2) in irradiated amorphous SiO_2. The STH_1 signal he observed was analogous to the one arising from the Ge-trapped hole observed by Hayes and Jenkin [8] while the STH_2 was assumed to arise from a hole trapped on two oxygen atoms. In addition to the ESR data, optical data for a STH in both Ge-doped α-quartz [10] and in amorphous SiO_2 [11] were also reported. On the theoretical side, the main efforts were concentrated on STE. Fisher *et al* [12] reported the first *ab initio* calculation of a STE in α-quartz using a Hartree–Fock (HF) method. Shluger and Stefanovich [13, 14] described the calculation for a STE in β-cristobalite by use of an approximate HF approach. The first *ab initio* HF calculation for the STH in amorphous SiO_2 has been reported recently by Edwards [15]. All these theoretical studies agree that the hole is located on an oxygen atom and that its two nearest-neighbour silicon atoms are found to relax away from the defect oxygen atom. The underlying problem with these calculations is the small size of cluster used. For example, in *ab initio* HF, only two silicon and seven oxygen atoms are included in the cluster although the cluster was embedded in an array of point charges. However, the hole localization is mainly due to polarization and distortion energy, both of which are long range in nature; further, many defect reactions can only be modelled by including many more atoms explicitly.

In the present work, we choose to use the classical static simulation package CASCADE [16] which can treat the polarization and distortion of a large cluster explicitly. The method incorporates the HADES code on which CASCADE is based, and has proved to be useful in the study of STH and its migration in alkali halide [17–20] and in the study of bipolarons in high-T_c superconductors [21]. In our calculation we used a larger cluster with 630 atoms and allowed all the atoms to be fully relaxed. We shall present results on the energies of STH, the lattice distortion caused by STH and the activation energy of STH in pure α-quartz.

2. Computational method

Our simulation is based on the shell model generalization of the Born model of the solid, which treats the solid as a collection of point ions with short-range repulsive forces acting between them. This approach has achieved a wide range of success, although, naturally, the reliability of the simulations depends on the validity of the potential model used in the calculations. Detailed discussion on this simulation technique can be found in [22]. Many of the key ideas and applications are given in the papers honouring 50 years of the Mott–Littleton method [23]. We shall only give a brief description of the interatomic potentials and defect energy calculation.

The short-range potentials used in this classic simulation are described by the Born–Mayer potential supplemented by an attractive r^{-6} term:

$$V(r) = A\exp(-r/\rho) - Cr^{-6} \tag{1}$$

where A, ρ and C are constants. The polarizability of individual ions and its dependence on local atomic environment is treated using the shell model [24], in which the outer valence cloud of the ion is simulated by a massless shell of charge Y and the nucleus and inner electrons by a core of charge X. The total charge of the ion is thus $X + Y$ which indicates the oxidation state of the ion. The interaction between the core and shell of any ion is treated as being harmonic with a spring constant k and represented by

$$V(r_i) = \tfrac{1}{2}k_i d_i^2 \tag{2}$$

where d_i is the relative displacement of core and shell of ion i. The electronic polarizability of the free ion i is thus given by

$$\alpha_i = Y_i^2/k_i. \tag{3}$$

The defect energy is defined as the energy to create a defect within the perfect lattice (for a full discussion of the terms involved, see [20]). In this work, we treated the defective lattice by using a two-region strategy [25]. In this approach the crystal is formally divided into an inner region (region I) and an outer region (region II). In the inner region the lattice configuration is evaluated explicitly while the outer region can be viewed from the defect as a continuum. The displacements within the outer region are due solely to the electric field produced by the total charge of the defect centred at the defect origin. The Mott–Littleton method [22] is employed in the outer region and the polarization P can be represented by

$$P = \frac{1}{4\pi}\left(1 - \frac{1}{\varepsilon_0}\right)\frac{ZeR}{R^3} \tag{4}$$

where ε_0 is the static dielectric constant of the solid and the R is the distance from the defect origin. In order to account consistently for the different treatment of the two regions, an interfacial region (region IIa) is introduced between region I and region II. This approach provides for the considerable relaxation of the crystal structure around the defect, and the total energy of the system can therefore be written as

$$E = E_{\mathrm{I}}(x) + E_{\mathrm{IIa}}(x, t) + E_{\mathrm{II}}(t) \tag{5}$$

in which $E_{\mathrm{I}}(x)$ is the energy of the region I, $E_{\mathrm{IIa}}(x, t)$ is the interaction energy between region I and II, and $E_{\mathrm{II}}(t)$ is the energy of region II. Here, the argument x is a vector of independent coordinates describing the region I, and t is the magnitude of a corresponding vector of the displacements in the region II.

In this work, the O ions are treated using the shell model while the Si ions are treated using a rigid model (without shell). We used the potential parameters A, ρ and C and shell parameters Y and k derived for the α-quartz by Sanders, Leslie and Catlow [26]. This potential includes a three-body interaction, and it reproduced the structure of α-quartz which is in good agreement with the experimental data and is successfully applied to calculation of the energies of point defects in quartz [27]. We used a radius of inner region of 10.4 Å which included 630 species and a radius of interfacial region of 22.4 Å which included 5612 species. All the ions in the two regions are fully relaxed in our calculation.

3. Results and discussion

3.1. Self-trapped hole

In our work we are mainly concerned with the problem of stability of a hole localized on an oxygen atom. It is *assumed* that the hole is on the oxygen, rather than being a prediction, so here we are using information from quantum chemistry. Two energy terms are involved in the self-trapping mechanism, the first being elastic energy and the other electronic energy. The elastic energy is contributed by lattice distortion as well as lattice polarization. Again, the polarization energy is composed of displacement and electronic components. We made an estimate of the two components of polarization energy arising from the localized hole on the oxygen atom by performing two calculations: (1) a 'thermal' calculation in which a full equilibrium of the lattice surrounding the defect is performed; (2) an 'optical' calculation in which only relaxation of the shells is allowed. The defect energies corresponding to the 'thermal' and 'optical' calculation are listed in table 1. We may equal the result of the second calculation to the partly electronic polarization energy surrounding the defect, while the difference between the optical and thermal calculations gives the displacement polarization energy. We note that the displacement polarization is substantial, with a value of about 8.5 eV, while the electronic polarization also has a large value of about 2.3 eV. We have also estimated the formation energy of a hole on an oxygen atom to be 12.64 eV, indicating that a great deal of energy is needed to form a hole on an oxygen atom. That the energy is so large is not a surprise, given the large bandgap (perhaps 10 eV) of quartz.

Table 1. The calculated defect energies in α-quartz.

	Energy (eV)		Displacement polarization energy (eV)	Electronic polarization energy (eV)	Hole formation energy (eV)
	Thermal	Optical			
O^- substituting at O^{2-}	21.39	29.72	8.33	2.31	12.64

We next proceed to calculate the total defect energy E_{vk} arising from a lattice distortion caused by a hole localized on the oxygen atom. In examining the stability of the self-trapped oxygen hole relative to a hole in its lowest-energy state in the valence band of an undistorted crystal, we follow the criterion proposed by Norgett and Stoneham [15] that the hole is self-trapped if the energy

$$E_s = E_{vk} + \tfrac{1}{2}E_v - E_M \tag{6}$$

is negative. Here E_{vk} is the calculated defect energy of the hole, E_v is the width of the valence band in the undistorted crystal, and E_M is the anion Madelung energy. In our case $E_{vk} = 21.39$ eV and $E_M = 31.80$ eV; the value of E_s can thus be estimated from

$$E_s = \tfrac{1}{2}E_v - 10.41 \text{ eV}. \tag{7}$$

The available experimental and calculated values of E_v for α-quartz are 20 eV [28] and 20 eV [29] respectively. We, therefore, use these values for the calculation in formula (7) and obtained E_s as -0.41 eV. The balance in energy is very close. The negative value of E_s indicates that self-trapping of a hole on an oxygen ion in α-quartz is possible. Self-trapping would be favoured still more had we allowed the silicon ions to polarize too. Although

our prediction is based on the difference between two large numbers, and so somewhat uncertain, the conclusion that the self-trapped state is slightly more stable is plausible. This calculation is believed to be the first calculation for a STH in pure α-quartz, although the STH in Ge-doped α-quartz [8] and in amorphous SiO_2 have been observed [9, 15].

We have also used the *ab initio* potential of α-quartz (this potential is referred to as potential B and the first potential we used is referred to as potential A) [30] to calculate the stability of the STH in α-quartz. The value of E_s calculated using potential B is 0.55 eV (see table 2) which is 0.8 eV higher than the value calculated using potential A. The difference in the E_s value is believed to arise from the difference between the dielectric constants of α-quartz calculated using the two different potentials. The dielectic constant calculated using potential B is not as good as the dielectric constant calculated using potential A (see [30]), although the two potentials give almost the same structural parameters and elastic constant. The dielectric constant plays an important role in defect calculation, with a small variation in its value resulting in a significant corresponding change in defect energy.

Table 2. The energy E_s of various SiO_2 polymorphs (negative E_s indicates the self-trapping of the hole).

		Energy E_s (eV)	
	Density (g cm^{-3})	Potential A	Potential B
α-quartz	2.649	−0.41	0.55
β-quartz	2.352	−0.09	0.83
α-cristobalite	2.344	0.42	0.95
β-cristobalite	2.174	0.99	1.49

We have used both potentials to calculate the stability of a STH in four polymorphs of silica (α-quartz, β-quartz, α-cristobalite and β-cristobalite). We found that α-quartz is most favourable for trapping a hole while β-critobalite is least favourable (see table 2). The plot of E_s against the density of the silicas is shown in figure 1. It is found that the denser the silica, the easier it is to trap a hole. For the amorphous silicas, the volume per molecular unit is systematically larger (density less) than for the crystalline silicas (see, e.g., figure 2 of [5]). This means that the variation of energy from site to site is critical for the amorphous silicas, whereas the average density is more significant in crystalline silicas.

3.2. Lattice distortion caused by a STH

Figure 2 and table 2 show core positions of some selected ions around the hole site before, and after, hole trapping. It is observed that trapping a hole on the O ion gives rise to the displacement of the oxygen ion O^- itself by 0.14 Å. However, the two nearest silicon ions Si(1) and Si(2) show large displacements of 0.40 Å and 0.63 Å respectively. It is noted that both Si(1) and Si(2) shift away from the central oxygen ion O^- and that the Si(2) ion shifts more than Si(1) ion. The other three oxygen ions surrounding the Si(2) ion (O(3), O(4) and O(6)) also show a large displacement compared to the three oxygen ions surrounding the Si(1) ion (i.e. O(1), O(2) and O(3)). The other six Si ions, Si(3), Si(4),... Si(8), which are further away from the central oxygen O^- ion, have relatively smaller displacements compared to the ions closer to the O^- ion. We also found the distance between the central O^- and its nearest-neighbour O ions increased, so we can rule out the possibility of the hole pulling two oxygen atoms together, as is seen in the V_K centre in alkali halides. We calculated the equilibrium geometries for the neutral charged cluster

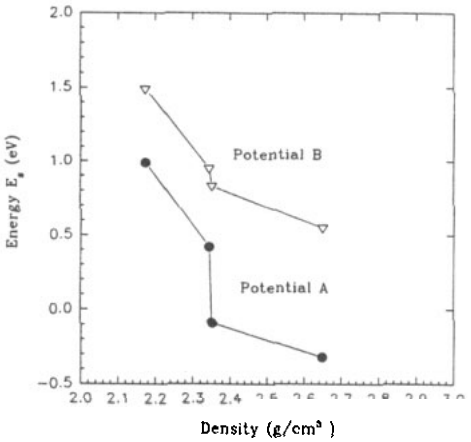

Figure 1. The variation of E_s with density of silicas. The forms shown are α-quartz, β-quartz, α-cristobalite and β-cristobalite.

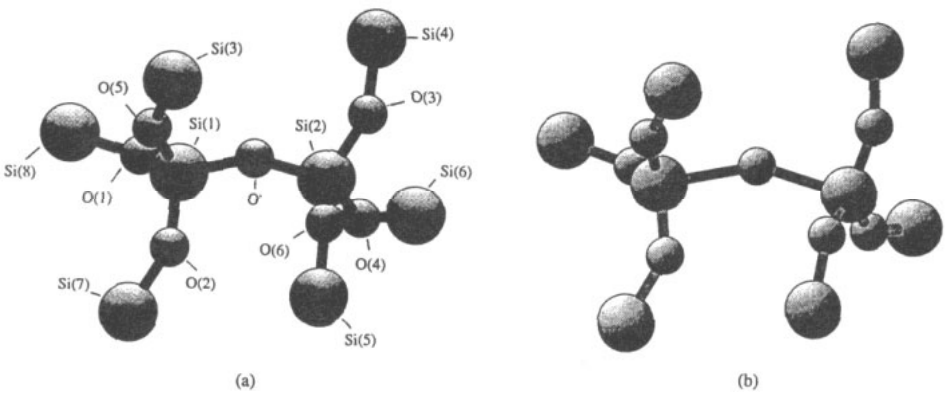

Figure 2. The geometry of the central part of (a) a neutral cluster and (b) a positively charged cluster. The differences in positions are analysed in the text.

(see table 4) and for the positively charged cluster, which correspond to the structure before and after hole trapping respectively. We found that both O^-–Si(1) and O^-–Si(2) bond lengths change significantly from about 1.6 Å for a neutral configuration to about 2.1 Å for a positively charged configuration. It is surprising to find that the bond angle of Si(1)–O^-–Si(2) undergoes only a very small change of about 1°, compared to the large elongation in the bond lengths of O^-–Si(1) and O^-–Si(2). We also calculated the bond length $R_{Si_{NN}-O_{NN}}$ and bond angle $\angle O_{NNN}$–Si_{NN}–O_{NNN} (where NN denotes the nearest neighbours and NNN next-nearest neighbours) with respect to the central O^- ion. It is found that after hole trapping, the bond length $R_{Si_{NN}-O_{NN}}$ shortened by about 0.4–0.5 Å while the bond angles $\angle O_{NNN}$–Si_{NN}–O_{NNN} increased by about 6–12° and bond angles $\angle O_{NNN}$–Si_{NN}–O_c (where O_c denotes the central O^- ion) decreased by about 8–15°. The bond lengths $R_{O_{NNN}-Si_o}$ (Si_o denotes the outer silicon ions) undergo an opposite change as compared to the bond lengths $R_{Si_{NN}-O_{NNN}}$ which *increase* by about 0.04–0.06 Å after hole trapping. The changes of the bond angles $\angle Si_{NN}$–O_{NNN}–Si_o show a different pattern. After hole trapping, the bond angles

∠Si(1)–O(5)–Si(3) and ∠Si(2)–O(3)–Si(4) increase, the bond angles ∠Si(1)–O(1)–Si(8) and ∠Si(1)–O(2)–Si(7) decrease, and the bond angles ∠Si(2)–O(6)–Si(5) and ∠Si(2)–O(4)–Si(6) remain almost unchanged.

Table 3. The core position before the hole is trapped at the O site (neutral position), the core position after the hole is trapped at the O site (relaxed position) and the displacement due to O trapping (all coordinates are given in ångströms).

	Neutral position			Relaxed positions			
Ion	X	Y	Z	X'	Y'	Z'	Displacement
O^-	0.000 03	0.000 10	0.000 02	−0.051 95	0.126 85	0.018 85	0.138 29
Si(1)	0.940 16	−1.126 26	0.650 89	1.160 40	−1.396 41	0.842 52	0.397 75
Si(2)	−0.081 03	1.122 41	−1.150 91	−0.118 89	1.624 64	−1.524 02	0.626 80
O(1)	0.000 03	−2.252 62	1.301 75	0.060 89	−2.370 11	1.372 28	0.149 94
O(2)	1.871 58	−1.757 62	−0.500 05	1.895 10	−1.814 64	−0.476 84	0.065 90
O(3)	−0.586 42	2.499 76	−0.500 05	0.625 55	2.768 15	−0.601 74	0.289 66
O(4)	−1.093 52	0.631 45	−2.301 85	−1.113 51	0.911 48	−2.491 68	0.341 44
O(5)	1.871 58	−0.494 90	1.801 82	1.926 18	−0.516 30	1.869 01	0.089 18
O(6)	1.364 48	1.373 41	−1.801 78	1.386 92	1.511 50	−1.905 74	0.174 30
Si(3)	2.376 97	0.882 45	2.452 69	2.412 35	0.915 46	2.487 48	0.059 60
Si(4)	−1.517 84	3.131 12	0.650 89	−1.573 65	3.220 62	0.674 55	0.108 10
Si(5)	2.376 97	0.882 45	−2.952 72	2.434 72	0.877 85	−3.016 63	0.086 26
Si(6)	−2.539 03	0.882 45	−2.952 72	−2.657 74	0.935 60	−3.047 95	0.161 20
Si(7)	2.376 97	−3.134 97	−1.150 91	2.426 85	−3.190 93	−1.209 35	0.095 05
Si(8)	−0.081 03	−3.374 93	2.452 69	−0.094 10	−3.516 43	2.549 73	0.172 08

We noted that after hole trapping the changes of the bond lengths O^-–Si(1) and O^-–Si(2) are about 30% while the changes of $R_{Si_{NN}-O_{NNN}}$ and $R_{O_{NNN}-Si_o}$ are only 2–3%. This indicates that the network relaxation is strongly localized on the three central ions (O^-, Si(1) and Si(2)), which is the same trend as that reported by Edwards [15]. Comparing our structural data with Edwards', we found the trend of the changes in the other structural parameters due to hole trapping to be the same, but our changes are somewhat larger than his [15]. Edwards [15] reported that network relaxation is comprised almost completely of the motion of the two silicon nearest neighbours away from the central oxygen. We found that some ions other than the three central ions can also experience quite large displacement as shown in table 2 (e.g. O(3) and O(4)). The difference between Edwards' data and ours is believed to arise from the fact that in Edwards' calculations only the inner seven oxygen atoms and two silicon atoms are allowed to relax, while in our calculation more than 630 species are allowed to relax fully.

The number of atoms inside the region I plays an important role in our defect calculation. If we include only 16 atoms in the region I then the defect energy E_{vk} is 22.87 eV. As the number of atoms inside the region I increases, the defect energy E_{vk} decreases (see figure 3). When we include 630 atoms, E_{vk} is 21.39 eV leading to the self-trapping of the hole. Including more atoms inside the region I also affects the displacement polarization energy and electronic polarization energy. If we use 16 atoms the displacement polarization energy and electronic polarization energy are 6.94 eV and 1.55 eV respectively, while when we use 630 atoms these values are increased to 8.33 eV and 2.31 eV respectively.

Table 4. Equilibrium geometry for the neutral and positively charged clusters shown in figure 1. Subscripts: c=central; NN=nearest neighbours; NNN=next-nearest neighbours; o=outer. The bond length is given in ångströms and the bond angle is given in degrees.

Bond length	Neutral	Positive	Bond angle	Neutral	Positive
$R_{O_c-Si_{NN}}$			$\angle Si_{NN}-O_c-Si_{NN}$		
O^-–Si(1)	1.6050	2.1139	∠Si(1)–O^-–Si(2)	143.98	143.03
O^-–Si(2)	1.6096	2.1513			
$R_{Si_{NN}-O_{NNN}}$			$\angle O_{NNN}-Si_{NN}-O_{NNN}$		
Si(1)–O(1)	1.6050	1.5613	∠O(1)–Si(1)–O(2)	110.71	116.71
Si(1)–O(2)	1.6096	1.5670	∠O(1)–Si(1)–O(5)	108.92	118.43
Si(1)–O(5)	1.6096	1.5539	∠O(2)–Si(1)–O(5)	109.29	118.44
Si(2)–O(3)	1.6050	1.5540	∠O(3)–Si(2)–O(4)	110.71	119.83
Si(2)–O(4)	1.6096	1.5630	∠O(3)–Si(2)–O(6)	108.35	120.94
Si(2)–O(6)	1.6050	1.5576	∠O(4)–Si(2)–O(6)	108.73	115.44
			$\angle O_{NNN} - Si_{NN}-O_c$		
O^-–O(1)	2.6018	2.8424	∠O(1)–Si(1)–O^-	108.29	100.24
O^-–O(2)	2.6158	2.7939	∠O(2)–Si(1)–O^-	108.79	97.65
O^-–O(3)	2.6158	2.7732	∠O(5)–Si(1)–O^-	110.71	97.58
O^-–O(4)	2.6255	2.8404	∠O(3)–Si(2)–O^-	108.92	95.56
O^-–O(5)	2.6447	2.7838	∠O(4)–Si(2)–O^-	109.29	98.52
O^-–O(6)	2.6447	2.7734	∠O(6)–Si(2)–O^-	110.71	95.46
$R_{O_{NNN}-Si_o}$			$\angle Si_{NN}-O_{NNN}-Si_o$		
Si(3)–O(5)	1.6050	1.6636	∠Si(1)–O(5)–Si(3)	143.98	153.27
Si(7)–O(2)	1.6050	1.6473	∠Si(1)–O(2)–Si(7)	143.98	138.48
Si(8)–O(1)	1.6096	1.6506	∠Si(1)–O(1)–Si(8)	143.98	137.84
Si(4)–O(3)	1.6096	1.6530	∠Si(2)–O(3)–Si(4)	143.98	147.85
Si(5)–O(6)	1.6096	1.6533	∠Si(2)–O(6)–Si(5)	143.98	143.63
Si(6)–O(4)	1.6050	1.6400	∠Si(2)–O(4)–Si(6)	143.98	143.30

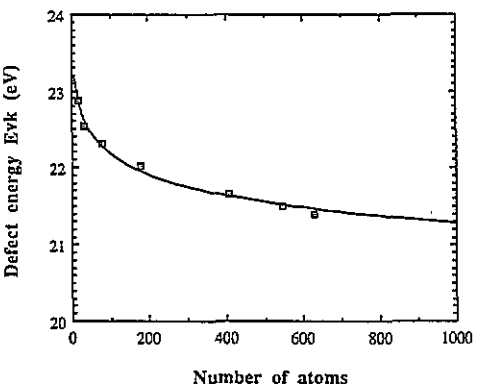

Figure 3. The variation of the defect energy E_{vk} with the number of atoms used in the calculation.

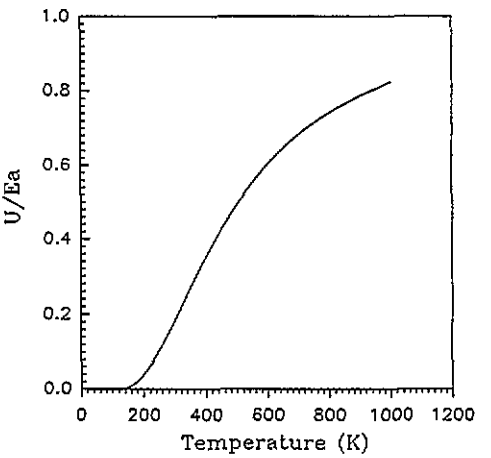

Figure 4. The ratio of the effective activation energy U to the calculated activation energy E_a, as a function of temperature. The curve is obtained from equation (9).

3.3. Calculation of activation energy of hole

3.3.1. Normal small-polaron hopping. At high temperatures the hopping rate of a hole is given by

$$W_{if} = \left(\frac{\pi}{4h^2 E_a kt}\right) |J_{if}|^2 \exp(-E_a/kT) \tag{7}$$

where E_a is the activation energy of a hole [18]. The activation energy E_a is the energy of the 'coincidence state' relative to the polaron ground state [2]. It can be expressed as the difference between the relaxation energy under the average of the initial and final forces, E_{av}, and the relaxation energy in the initial configuration E_i [18]

$$E_a = E_{av} - E_i. \tag{8}$$

We calculate the E_{av} to be 27.06 eV and E_i to be 21.39 eV. The activation energy E_a is then estimated to be 5.67 eV, which is far larger than the expected value of a few tenths of an eV.

There are two possible explanations. The first is that expression (7) is only valid at high temperatures, i.e. $\hbar\omega/kT < 1$ where ω is angular frequency of a phonon and T is temperature. Because the experiment is usually undertaken at low temperatures, we need to estimate a corresponding 'effective activation energy' U, which is related to the experimental data. The effective activation energy U is given by [18]

$$U = E_a 2\,\mathrm{cosech}^2(y)\left(\frac{I_1[S\,\mathrm{cosech}(y)]}{I_0[S\,\mathrm{cosech}(y)]}\cosh(y) - 1\right) \tag{9}$$

where I_0 and I_1 are modified Bessel functions, $y = \hbar\omega/kT$ and $S = 4E_a/\hbar\omega$. The formula (9), with ω equal to the longitudinal optical frequency, is usually used to relate the calculated E_a to the experimental data [18, 19]. Using the experimental value $\nu = \omega/2\pi = 36.7$ THz [31], we obtained the ratio U/E_a (shown in figure 4). It is seen that U/E_a is temperature dependent. At $T = 180$ K, $U/E_a = 0.0215$. This yields the effective activation energy of 0.122 eV, which is about half the energy needed to self-trap a hole on an oxygen ion. We note that below 120 K, U/E_a is close to zero, leading to a calculated effective activation energy U close to zero. This implies that at very low temperatures (say $T = 120$ K) the activation energy of a hole is very small, so the hopping rate of the hole will be fast enough to prevent the observation of stable long-term self-trapping. This result seems to agree with experimental results [8], i.e., in crystalline quartz at 4 K the hopping rate of holes is still fast enough to prevent stable long-term self-trapping of the type of hole found in more ionic solids such as alkali halides.

3.3.2. An alternative mechanism. Since the coincidence state energy (E_a) is predicted to be very high, the obvious question is whether the standard small-polaron hopping mechanism is appropriate. As has been noted for other oxides (especially NiO, [2]), charge transport could proceed via the small polaron being excited to the mobile large-polaron state. This would have a lower activation energy, of the order of the few tenths of an eV, which we have calculated, corrected for the lattice deformation in the large-polaron state. Experimentally, this would lead to differences in thermopower, but this is academic in the present case where experiments are unlikely to succeed. If the small polaron is indeed stable by such a small amount, we should expect that there will be populations of both small and large polarons, and it is the behaviour of this mixed population whose properties are observed.

4. Conclusions

We have investigated the possibility of STH existing in pure α-quartz by using the classic defect simulation technique. It is found that the hole can be self-trapped in an oxygen ion with a binding energy of 0.41 eV. The STH gives rise to a large displacement polarization energy of 8.43 eV and a large electronic polarization energy of 2.31 eV. The STH is accompanied by a localized network distortion wherein the O^- ion, on which the hole is self-trapped, shifts by 0.14 Å and the nearest-neighbour silicon atoms move 0.4–0.6 Å away from the O^- ion. This result is similar to the *ab initio* HF calculation of STH in amorphous SiO_2. We also calculated the activation energy of STH and estimated the effective activation energy to be 0.12 eV at 180 K. This small activation energy of STH may imply that the hopping rate of the hole will be fast enough to prevent stable long-term self-trapping. However, the low self-trapping energy does suggest that small- and large-polaron populations should coexist. The self-trapped holes may therefore be bound to defects unless there is extra stabilization from other causes, e.g. in amorphous silicas or where image interaction favours localization too.

References

[1] Shluger A L and Stoneham A M 1993 *J. Phys.: Condens. Matter* **5** 3049
[2] Stoneham A M 1989 *J. Chem. Soc. Faraday Trans. II* **85** 505
[3] Landau L 1933 *Phys. Z. Sowjetunion* **3** 664
[4] Hagon J P, Jaros M and Stoneham A M 1985 *J. Phys. C: Solid State Phys.* **18** 4957
[5] Stoneham A M 1991 *Insulating Films on Semiconductors* ed W Eccleston and M Uren (Bristol: Institute of Physics) p 19
[6] Ong C K, Harker A H and Stoneham A M 1993 *Interface Sci.* **1** 139
[7] Stesmans A and Vanheusden K 1991 *Phys. Rev.* B **44** 11 353
[8] Hayes W and Jenkin T J L 1986 *J. Phys. C: Solid State Phys.* **19** 6211
[9] Griscom D L 1992 *J. Non-Cryst. Solids* **149** 137
[10] Jenkin T J L, Koppitz J, Schirmer O F and Hayes W 1987 *J. Phys. C: Solid State Phys.* **20** L367
[11] Chernov P V, Dianov E M, Karpechev V N, Kornienko L S and Sulimov V B 1990 *Phys. Status Solidi* b **155** 663
[12] Fisher A J, Hayes W and Stoneham A M 1990 *Phys. Rev. Lett.* **64** 2667; *J. Phys.: Condens. Matter* **2** 6707
[13] Shluger A L 1988 *J. Phys. C: Solid State Phys.* **21** 431
[14] Shluger A L and Stefanovich E 1990 *Phys. Rev.* B **42** 9664
[15] Edwards A H 1993 *Phys. Rev. Lett.* **71** 3190
[16] Leslie M 1982 *SERC Daresbury Laboratory Technical Memorandom No* DL/SCI/TM31-T
[17] Norgett M J and Stoneham A M 1973 *J. Phys. C: Solid State Phys.* **6** 229
[18] Norgett M J and Stoneham A M 1973 *J. Phys. C: Solid State Phys.* **6** 238
[19] Monnier R, Song K S and Stoneham A M 1977 *J. Phys. C: Solid State Phys.* **10** 4441
[20] Cade P E, Stoneham A M and Tasker P W 1984 *Phys. Rev.* B **30** 4621
[21] Zhang X and Catlow C R A 1991 *J. Mater. Chem.* **1** 233
[22] Catlow C R A and Mackrodt W C (ed) 1982 *Computer Simulation of Solids (Springer Lecture Notes in Physics 166)* (Berlin: Springer)
[23] 1989 *J. Chem. Soc. Faraday Trans. II* **5**
[24] Dick B G and Overhauser A W 1958 *Phys. Rev.* **112** 90
[25] Norgett M J and Lidiard A B 1972 *Computational Solid State Physics* ed F Herman *et al* (New York: Plenum) p 385
[26] Sanders M J, Leslie M and Catlow C R A 1984 *J. Chem. Soc. Chem. Commun.* **1271**
[27] Leslie M 1989 *J. Chem. Soc. Faraday Trans. II* **85** 407
[28] Olivier J, Faulconnier P and Poirier R *Physics of SiO_2 and its Interfaces* ed S T Pantelides (New York: Academic) p 93
[29] Calabrese E and Fowler W B 1978 *Phys. Rev.* B **18** 2888
[30] Purton J, Jones R, Catlow C R A and Leslie M 1993 *Phys. Chem. Minerals* **19** 392
[31] Strauch D and Dorner B 1993 *J. Phys.: Condens. Matter* **5** 6149